

Experiments on the water entry and/or exit of a cone

Alan Tassin, Thibaut Breton, Nicolas Jacques

▶ **To cite this version:**

Alan Tassin, Thibaut Breton, Nicolas Jacques. Experiments on the water entry and/or exit of a cone. International Workshop on Water Waves and Floating Bodies (IWWWFB), Apr 2018, Guidel-plage, France. hal-01864856

HAL Id: hal-01864856

https://ensta-bretagne.hal.science/hal-01864856

Submitted on 30 Aug 2018

HAL is a multi-disciplinary open access archive for the deposit and dissemination of scientific research documents, whether they are published or not. The documents may come from teaching and research institutions in France or abroad, or from public or private research centers.

L'archive ouverte pluridisciplinaire **HAL**, est destinée au dépôt et à la diffusion de documents scientifiques de niveau recherche, publiés ou non, émanant des établissements d'enseignement et de recherche français ou étrangers, des laboratoires publics ou privés.

Experiments on the water entry and/or exit of a cone

Alan Tassin[1]*, Thibaut Breton[1,2], Nicolas Jacques[2]
[1]IFREMER, Marine Structures Laboratory, Z.I. Pointe du Diable, France
[2]ENSTA Bretagne, FRE CNRS 3744, IRDL, 29806 Brest Cedex 09, France
***alan.tassin@ifremer.fr**

1 Introduction

We report on recent experiments of water exit and combined water entry and exit. The water exit phenomenon refers to the lifting of a body initially floating at the water surface (pure exit) or to the lifting of a body just after a water entry phase (combined water entry and exit). Water exit is relevant to different fields of applications (e.g. marine and naval engineering, aeronautics, biomechanics) and is known for generating suction loads on structures. This work is the continuation of the first experiments presented in Tassin et al. (2017a) and Tassin et al. (2017b) dedicated to the water exit of flat plates. The experimental approach investigated previously is now extended to three-dimensional bodies such as a cone with a deadrise angle of 15° and to mock-ups of bigger scale (up to 50 cm diameter). In particular, the LED edge-lighting previously used to illuminate the contact line during the water exit of a transparent modified square plate has been adapted to the tracking of the contact line during the water exit of a transparent conical shell. New water exit experiments were also carried out with a circular disc of 40 cm diameter in order to study the influence of the body shape. We also performed combined water entry and exit experiments with a conical mock-up in order to investigate the performance of the LED edge-lighting technique for the tracking of the contact line during the entry stage. Following our previous work (see Tassin et al. (2017a)), the accuracy of the LED edge-lighting technique during cone water exit was assessed through comparison with experiments during which a draughtboard was placed at the bottom of the tank.

2 Experimental set-up

The experiments were carried out in the current-wave flume of IFREMER located in Boulogne-sur-Mer (France). A sketch of the experimental set-up is drawn in Fig. 1. One can see a transparent mock-up (here a circular disc) made out of PMMA fixed to a metallic frame. A high-speed (1000 fps) video camera (Photron FastCam Mini AX50 fitted with a 20 mm lens) looking downwards is fixed to the metallic frame and the metallic frame is fixed to a 6 DOF motion generator. The motion generator is suspended above the water tank and is used to generate a vertical motion with minimum pitch and roll angles. The water tank is 2 m deep, 4 m wide and 20 m long, which is significantly bigger than the water tank used in the previous experiments (Tassin et al. (2017a)). A sketch of the 15° transparent conical shell is shown in Fig. 2. The thickness of the shell in the central part is 15 mm. A high-power LED ribbon/array covered of aluminium sellotape is fixed along the edge of the mock-up. In order to calibrate the optical system and to be able to measure the radius of the wetted surface, we manufactured a 3D calibration part over which a vertical projection of a square grid was printed. The calibration set-up used for a spherical mock-up is illustrated in Fig. 3. A similar calibration set-up was manufactured for the conical mock-up. The calibration part was elevated until being in contact with the lower surface of the mock-up before the experiments in order to calibrate the images. Starting from rest ($z = 0$, $\dot{z} = 0$, $\ddot{z} = 0$), the motion imposed to the mock-up during the water exit experiments was of the following form:

$$\begin{cases} z(t) = H[1 + \mathrm{erf}(U_{max}(t - t_0)\sqrt{\pi}/H)]/2, & z \leq H \\ \dot{z}(t) = U_{max}, & z \geq H/2, \end{cases} \tag{1}$$

where $\mathrm{erf}(x) = 2/\sqrt{\pi}\int_0^x \exp(-\tau^2)\mathrm{d}\tau$ is the error function, z is the vertical position of the mock-up and U_{max} is the maximum vertical velocity. The parameters H and U_{max} were adjusted according

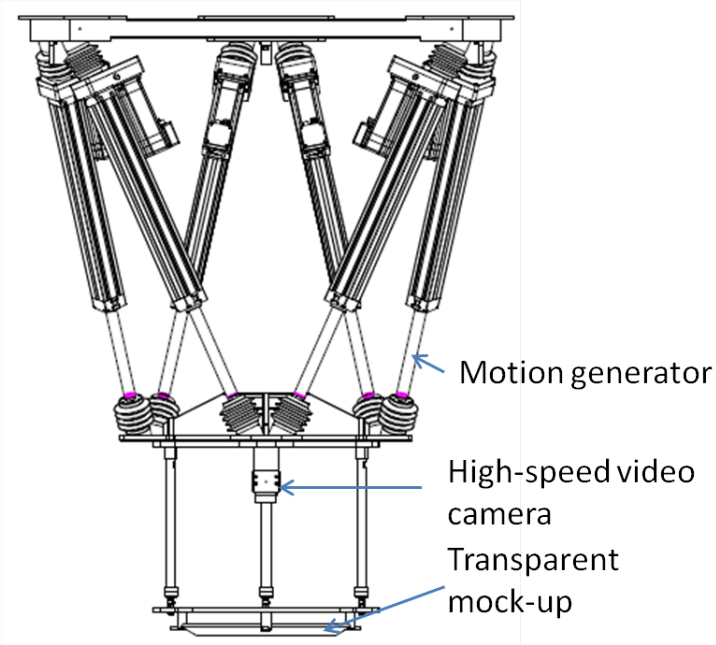


Figure 1: Description of the experimental set-up

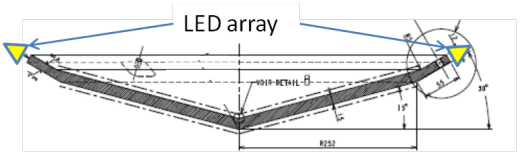


Figure 2: Vertical cross-section of the conical mock-up

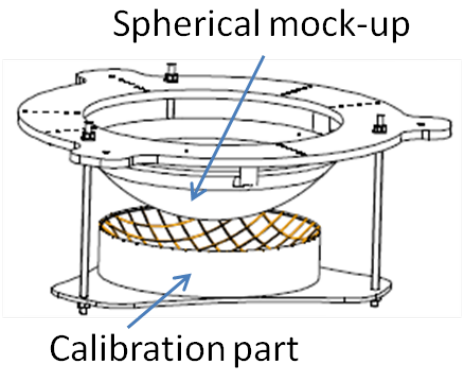


Figure 3: Sketch of the calibration grid used for the spherical mock-up

to the limits of the motion generator in terms of velocity, acceleration and power. In the following, $H = 10$ cm, $U_{max} = 0.6$ m/s and the reference time t_0 is such that $z(t = 3\text{ s}) = H/2$. Note that the form of the motion was inspired from the work of Reis et al. (2010) dedicated to the cat lapping phenomenon. During the combined water entry and exit experiments, the motion imposed to the mock-up was of the following form:

$$\begin{cases} z(t) = -H\sin(2\pi t/T), & t \leq T/2 \\ \dot{z}(t) = U_{max}, & t \geq T/2, \end{cases} \tag{2}$$

with $T = 2\pi H/U_{max}$, $U_{max} = 0.6$m/s and H is the maximum penetration depth. The evolution of the target velocity, $\dot{z}(t)$, and acceleration, $\ddot{z}(t)$, are depicted in Figs. 4 and 5 below.

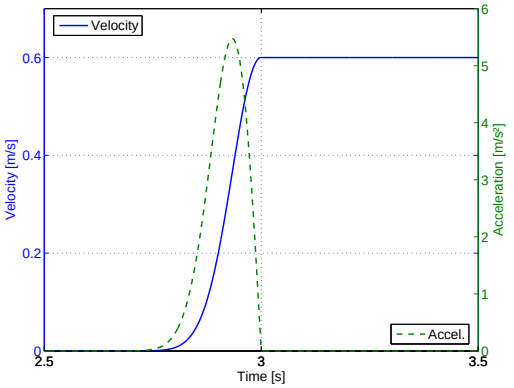


Figure 4: Target velocity and acceleration for the cone water exit

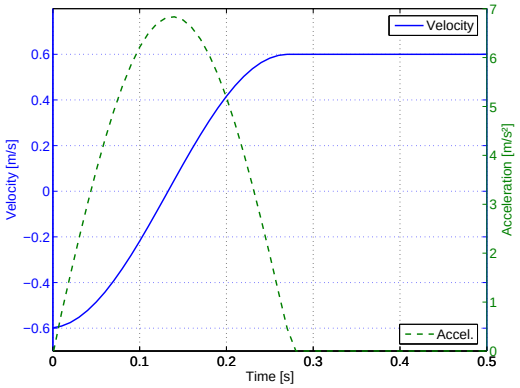
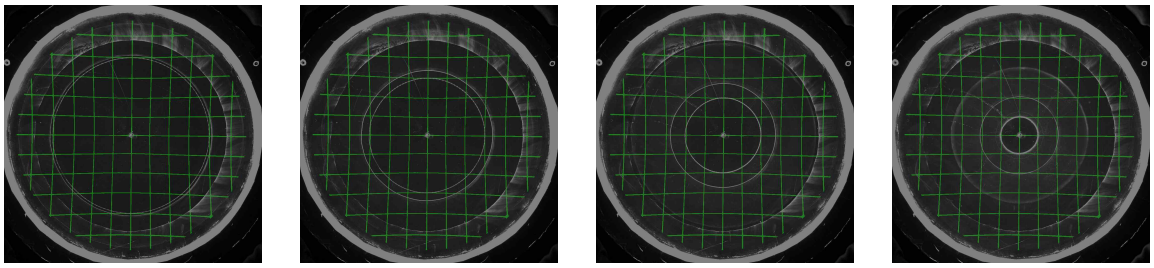


Figure 5: Target velocity and elevation for the cone water entry and exit

3 Results

A sequence of images obtained during an experiment of water exit with the conical mock-up is plotted in Fig. 6. A binarised image (in green) of the calibration grid has been superimposed to the images of the cone. The horizontal spacing between the grid lines is 42 mm. Similarly to the results obtained with a circular disc in Tassin et al. (2017b), one can observe a luminous contour which contracts towards the centre of the mock-up as time increases. In order to demonstrate that the illuminated contour delimits the surface of contact between the liquid and the cone, we also performed experiments during which a draughtboard was placed at the bottom of the water tank (about 2 m deep). A sequence of images obtained with the draughtboard technique, and for similar time instants as in Fig. 6, is plotted in Fig. 7. This comparison clearly shows the correspondance between the illuminated contour and the perimeter of the surface over which the draughtboard is "undistorted" (there is still some distorsion due to the cone shape). For the sake of comparison, a sequence of images obtained during the water exit of a circular disc is plotted in Fig. 8. A binarised image of the calibration grid (in green) has also been superimposed to the images of the disc. The horizontal spacing between the grid lines is 30 mm in this case. Note that during this experiment the motion of the disc is similar to the motion of the cone, so it is possible to compare Fig. 8 to Figs. 6 and 7. In Fig. 8, we can see that the distortion of the calibration grid is much smaller than in Fig. 6. The evolution of the contact line during the water exit of the disc is rather close to the evolution of the contact during the water exit of the cone, but the shape of the contact line starts to deviate from a circle at the end of the disc experiment (Fig. 8d). This distorsion may be due to an instability or to imperfect initial conditions (non-circular initial wetted surface). The conical mock-up was also used to carry out combined water entry and exit experiments. For this purpose, the maximum penetration depth H in Eq. 2 was set such that the theoretical maximum radius of the contact line predicted by the Wagner model ($c_{max} = 4H/(\pi \tan 15°)$) should be equal to 25 cm. A sequence of images obtained during the water entry and exit of a cone with a deadrise angle of 15° is plotted in Fig. 9. During the entry stage (Figs. 8a and 8b), one can observe both the contact line (or turn-over line) and the jet front. During the exit stage (Figs. 8c and 8d), the contact line is also clearly visible.

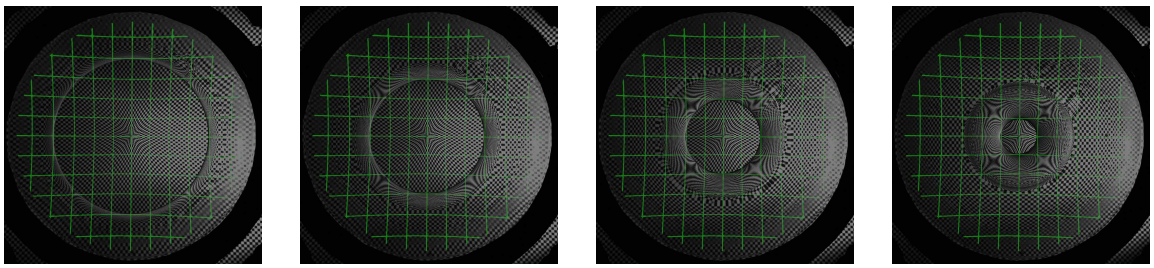


(a) t=2.953 s (b) t=3.006 s (c) t=3.064 s (d) t=3.138 s

Figure 6: Sequence of images obtained during the water exit of a cone. The diameter of the wetted surface is initialy equal to 40 cm.

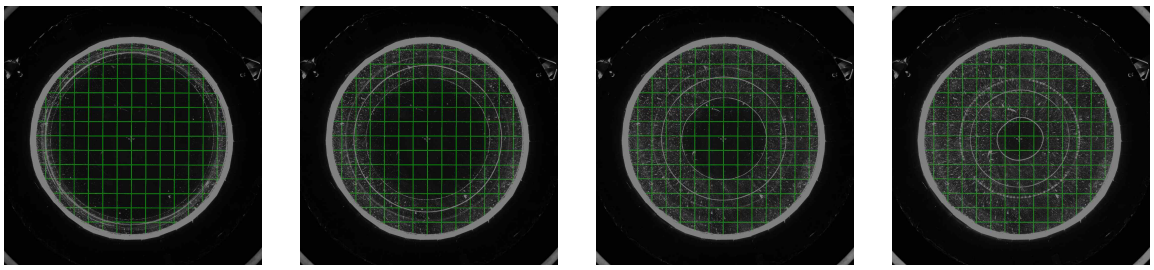
4 Conclusion and discussion

The LED edge-lighting technique has been successfully used to track the contact line during the water exit of a cone and during the combined water entry and exit of a cone. We have demonstrated that the edge-lighting technique could be used in a medium scale wave tank with mock-ups of 50 cm diameter. The technique also makes it possible to follow the jet front which is formed during the entry stage, which is not possible with the classical technique of bottom views with opaque mock-ups. The LED edge-lighting technique could therefore be of interest for the study of liquid ejecta during water impacts (see Marston and Thoroddsen (2014)). The images and results have been obtained very recently and are still being process. More detailed analyses will be presented at the workshop. We also plan to run CFD simulations of the experiments. A series of experiments (water exit, water entry and exit, wave



(a) t=2.953 s (b) t=3.006 s (c) t=3.064 s (d) t=3.138 s

Figure 7: Sequence of images obtained during the water exit of a cone with the draughtboard technique. The diameter of the wetted surface is initialy equal to 40 cm.



(a) t=2.953 s (b) t=3.006 s (c) t=3.064 s (d) t=3.138 s

Figure 8: Sequence of images obtained during the water exit of a 40cm diameter circular disc.

impact) have been carried out with a spherical mock-up and will be presented at the workshop.

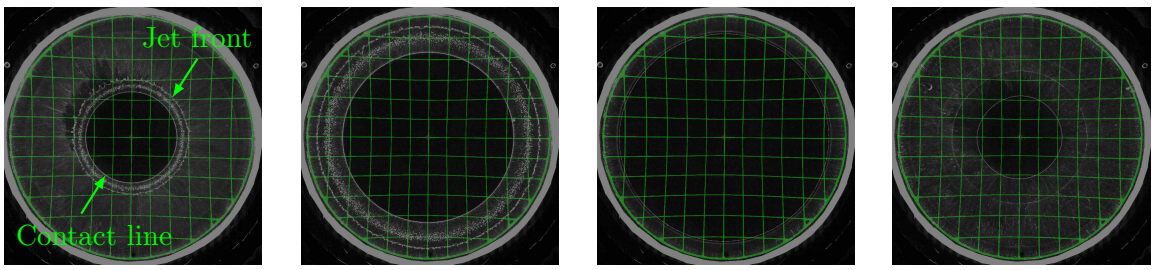
References

Marston, J. and Thoroddsen, S. T. (2014). Ejecta evolution during cone impact. *Journal of Fluid Mechanics*, 752:410–438.

Reis, P. M., Jung, S., Aristoff, J. M., and Stocker, R. (2010). How cats lap: Water uptake by felis catus. *Science*, 330:1231–1234.

Tassin, A., Breton, T., Forest, B., Ohana, J., Chalony, S., Le Roux, D., and Tancray, A. (2017a). Visualization of the contact line during the water exit of flat plates. *Experiments in Fluids*, 58(8):104.

Tassin, A., Breton, T., and Jacques, N. (2017b). Evolution of the contact line during the water exit of flat plates. In 32nd *International Workshop on Water Waves and Floating Bodies*, 23-26 April 2017, Dalian, China.



(a) t=67 ms (b) t=104 ms (c) t=197 ms (d) t=349ms

Figure 9: Sequence of images obtained during the water entry (a,b) and exit (c,d) of a cone